applied sciences

MDPI

Review

A Review: Factors Affecting Internal Two-Phase Flow-Induced Vibrations

Umair Khan, William Pao * and Nabihah Sallih

Mechanical Engineering Department, Universiti Teknologi PETRONAS (UTP), Seri Iskandar 32610, Malaysia
* Correspondence: william.pao@utp.edu.my

Abstract: Two-phase flow is commonly encountered in various engineering systems. Momentum fluctuation in two-phase flow can create undesirable and destructive vibrations. These vibrations are known as flow-induced vibrations, which are a fundamental phenomenon in fluid–structure interactions, and have been the center of this type of research in the past few decades. Flow-induced vibrations due to the multiphase flow are a complex phenomenon and its understanding is still immature. Various accidents related to flow-induced vibrations have been reported in heat exchangers and piping systems and it is very important to develop a deeper understanding of flow-induced vibrations in multiphase flow. The present review article aims to discuss the literature related to flow-induced vibrations, with special focus on factors affecting flow-induced vibrations in internal two-phase flow. Various factors affecting the magnitude and dominant frequency of forces are narrated and the correlations previously developed to estimate these quantities are discussed. Dimensionless forces are extracted from the literature and plotted against Weber number, to provide a database for comparison and to serve as a validation tool for any studies conducted using computational fluid dynamics. Furthermore, some important literature on flow-induced vibrations under different conditions is presented in tabular form to better understand these findings. Finally, some concluding remarks and comments on future research prospects and challenges are outlined.

Keywords: flow-induced vibrations; dimensionless forces; dominant frequency; Weber number; fluid–structure interaction

Citation: Khan, U.; Pao, W.; Sallih, N. A Review: Factors Affecting Internal Two-Phase Flow-Induced Vibrations. *Appl. Sci.* **2022**, *12*, 8406. https://doi.org/10.3390/app12178406

Academic Editor: Jianzhong Lin

Received: 12 July 2022
Accepted: 19 August 2022
Published: 23 August 2022

1. Introduction

Fluid flow is an important phenomenon in many engineering systems. In the literature, primarily two different flows are discussed, namely single-phase and multiphase flows. Two-phase flow is a simplified form of multiphase flow, which is further classified into gas–liquid [1], liquid–liquid [2,3], gas–solid [4,5], and liquid–solid flow [6,7]. It is widely present in various engineering systems, such as petroleum transportation and production, power plants, chemical industry, and heat exchangers. Moreover, two-phase flow is very unstable due to its fluctuating density, pressure, velocity, and momentum [8,9]. This fluctuating nature of two-phase flow, when combined with bends used to change the flow direction, can produce gravitational, centrifugal, and buoyant forces [10,11]. This leads to a complex fluid–structure interaction (FSI), which causes severe vibrations. These vibrations have recently attracted considerable attention and are known as flow-induced vibrations (FIV).

Fluid-related vibrations were discussed in the two conferences [12,13] held in 1972 and 1979 in Germany. Several practical problems in the field of fluid-related vibrations and their results were presented. The term, FIV, became well-known after it was coined by Blevins [14] in his book. Flow-induced vibrations can be explained as a form of sequential interaction between hydrodynamic forces and structural dynamics. The fluid exerts force on the surface of structure, causing the structure to deform. The deformation of the structure depends on the mechanical properties of the structure. In response, the deformed structure will react and apply the opposite force against the fluid. Consequently, flow-induced vibration is generated due to the interaction between these two forces, according to Blevins [15]. Furthermore, for the first time, Blevins classified FIV based on two types of flows, namely steady and unsteady flows. Later, the types of FIV already known were classified based on the type of flow involved [16], as shown in Figure 1. In steady flow, the interaction between fluid and structure is the main cause of vibration forces, whereas in unsteady flow, turbulent forces are the main source of vibrations.

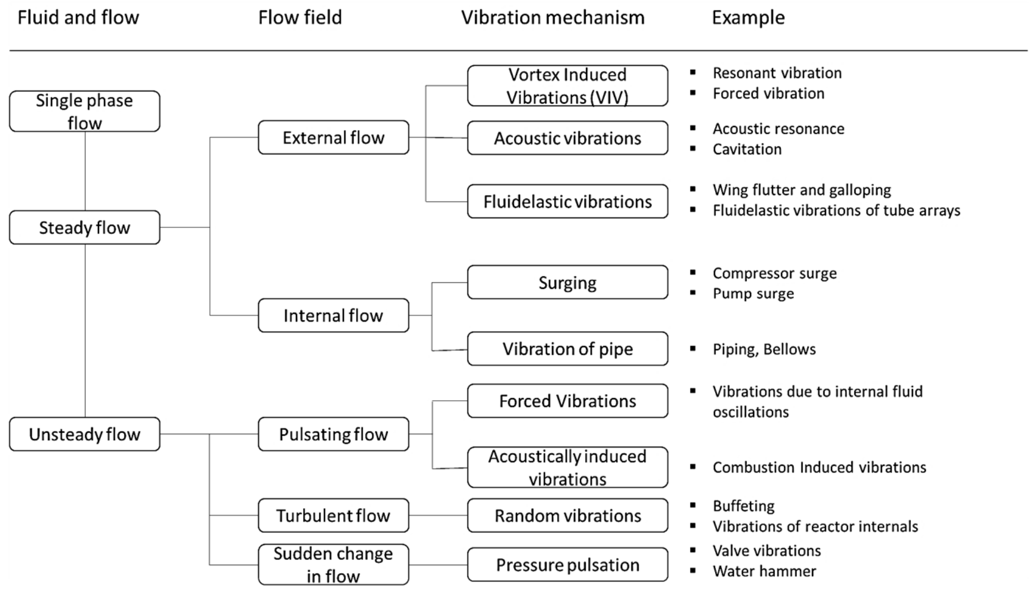

Figure 1. Classification of flow-induced vibrations.

The focus of this review is FIV due to the two-phase flow. Two-phase FIV can be divided into three categories [16], as illustrated in Figure 2. The first category is the vibration of piping system by the two-phase flow, which includes FIV generated due to the impact of flow or change in flow direction as a result of piping components, such as bends and T-junctions. The second category, bubble-induced vibration, is primarily due to the sloshing effect. The third category, thermal-hydraulic vibration associated with phase change, induced from the main sources of the FIV process, involves phase change due to the energy transfer between the interface, such as the instability caused by boiling and condensation. Examples of thermal-hydraulic vibration include flow in suppression pool and feedwater piping of nuclear power plant. Moreover, vibrations generated by the two-phase flow can be categorized based on flow orientations, namely internal and external flow. Flow-induced vibrations due to internal and external flows are discussed in the next section.

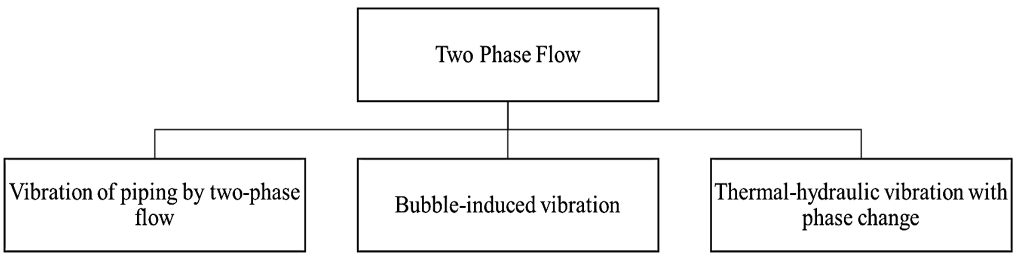

Figure 2. Classification of two-phase flow-induced vibrations.

1.1. Two-Phase External Flow

Two-phase external flow indicates that the fluid is flowing outside a pipe or a bundle of pipes. Major causes of FIV due to external flow include vortex-induced vibrations (VIV) [17], vortex shedding, and fluid-elastic vibrations [14]. In the past few decades, FIV due to external flow has been studied by many researchers [18–21]. For example, Kang et al. [18] developed a model to examine the effect of spring support on FIV due to external axial flow. In addition, Shiels et al. [20] studied the effect of flow-induced vibrations on circular cylinder due to external cross flow. Two main types of external two-phase flow are explained in the following sub-sections.

1.1.1. Axial Flow

External axial flow is defined as the flow of fluid parallel to the axial direction of pipe and it is also known as parallel flow, as shown in Figure 3a. Geometries, such as straight tubes or tube bundles, when subjected to axial flow at high velocities, may undergo some instabilities. These instabilities can be generated at low velocities due to pressure fluctuations. Vibrations due to external axial flow are usually smaller than in the case of external cross flow. Considerable studies have been performed on axial-flow-induced vibrations, especially since the surfacing of nuclear reactors in 1960s, focusing on systems, such as Boiling Water Reactor fuel bundles, are subjected to axial flow [22,23]. The vibration due to axial flow is mainly due to vibration mechanisms, such as fluid elastic instabilities and random turbulence excitations [24–27]. Void fraction fluctuations, flow velocity, pressure, and geometry are reported to be major influencing parameters. Pettigrew and Taylor [28] reported that based on their experimental work on BWR fuel rod under steam water flow, there is no effect on vibration due to nucleate boiling on the surface of the heated rod. Kang et al. [18] proposed a model for axial-flow-induced vibrations to examine the effect of spring support on FIV for Pressurized Water Reactor fuel rods. The vibration response for both spring supported and simply supported rods was recorded. The displacement in the case of spring supported rod was larger than the simply supported rod, and vibration displacement decreased with the increasing spring constant for the spring supported rod. Gorman [29] reported from his experiments on BWR fuel rod vibrations that damping in axial flow is approximately four times higher compared to the single-phase flow. Moreover, the author reported that the highest amplitude of vibrations was observed for mass quality (vapor mass/total mass) range of 0.1 and 0.2. Later, Pettigrew and Gorman [30] also reported a peak amplitude at mass quality of 0.1–0.2 and 0.4–0.5, indicating the role played by flow regime on vibration amplitude, considering flow regime changes with the change in mass quality. The effect of flow regime was not properly explained, and it is hard to create a linkage of two-phase flow regime with axial FIV [31,32].

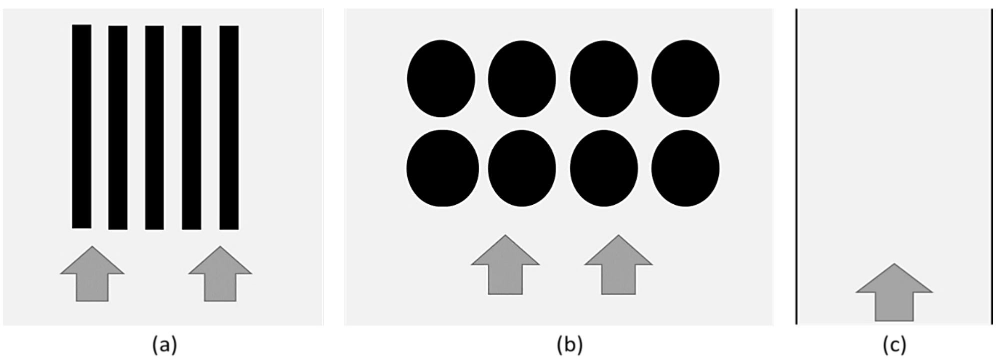

Figure 3. Types of two-phase flow. (**a**) Axial flow, (**b**) cross flow, (**c**) internal flow.

1.1.2. Cross Flow

Cross flow is another type of flow, where fluid flows perpendicular to a group of pipes, as shown in Figure 3b. This type of flow involves isolated cylinders as well as bundles of cylinders. It is commonly found in submerged legs of offshore structures, shell and tube heat exchangers, nuclear steam generators, and petrochemical industries [33–38]. Flow-induced vibrations due to cross flow are generated by mechanisms, such as fluid elastic instabilities, vortex excitation, periodic wave shedding, bubbles and structure interaction, and random excitation caused by turbulence [39–42]. Flow-induced vibrations can be severe under resonance conditions. However, Shiels et al. [20] reported that FIV due to cross flow on a cylinder can be with significantly higher amplitudes even without the presence of coupling with mechanical system, which can cause resonance. These vibrations depend on many factors, such as configuration of cylinders, physical properties of fluid, pitch to diameter ratio, Reynold number, flow velocity, flow regime, and turbulence level [43,44].

1.1.3. Two-Phase Internal Flow

Two-phase internal flow is the most common type of flow in oil and gas, chemical industries, and numerous engineering systems. In this flow, fluid flows inside the pipe as shown in Figure 3c. FIV in two-phase internal flow has attracted considerable attention due to high instabilities and complex interactions at interface. Flow turning elements causing a sudden momentum change and pressure fields change are the main reason for FIV in internal two-phase flow [45–52]. Different factors affecting FIV in internal two-phase flow, such as geometry, flow pattern, velocity, and void fraction, are discussed in detail in the next section. Various correlations are developed over time to calculate flow-induced vibrations in different geometries, which are further explained in Section 4. These correlations mainly focus on determining dimensionless forces and dominant frequency. Computational fluid dynamics methods are instrumental in FIV research and many scholars [53–56] have clearly verified the use of VOF model to handle multiphase flow patterns and turbulence inside the pipe. With the development of computational methods, many researchers have implemented one-way and two-way FSI models to study fluid–structure interactions in pipes with bends [57–61]. Moreover, different studies have been conducted to study the displacement due to vibration.

Miwa et al. [62] published a review paper which explains FIV in internal two-phase flow. However, the authors were more focused on developing a correlation to determine the forces on bend. In contrast, the present review paper discusses various parameters affecting the magnitude and frequency of the forces causing these vibrations, in addition to the inclusion of the most recent literature. Moreover, the relationship between different influencing parameters and dominant frequency of forces is discussed. A detailed comparison of dimensionless forces against Weber number is performed, which is helpful in comparing the major works performed in this field. These data can be used to easily validate the accuracy of CFD results with previous experimental results. Different correlation models developed in the past are collected and discussed, along with up-to-date models presented in the literature. An overview of the work performed on two-phase internal flow-induced vibrations is listed in Section 4.

2. Factors Affecting FIV in Internal Two-Phase Flow

The first experiment to relate momentum fluctuation with FIV was conducted by the authors of [8]. In this experiment, effects of volumetric quality, flow velocity, pressure, flow channel size, and geometry were observed. In the next section, the effects of different parameters are discussed in detail.

2.1. Effect of Flow Velocity

The effect of flow velocity on FIV was reported in research conducted on multiphase FIV at bends with 20.6 mm internal diameter [48,63]. A piezoelectric force sensor was used to record excitation force signal and an optical probe was used to record void fraction data. It was reported that the amplitude and predominant frequency of excitation forces increase linearly with flow velocity, for a given void fraction. As the velocity of the fluid increases, the higher modes become excited. Moreover, the authors correlated the root mean square of excitation force (F_{RMS}) with inlet superficial mixture velocity (V_m). The experimental results on U-bends suggested that the relationship between excitation forces and superficial velocities can be expressed in Equation (1), as shown below:

$$F_{RMS} \propto {V_m}^{1.2} \quad (1)$$

The same trend was also reported by Giraudeau et al. [64]. The authors conducted experiments to investigate FIV for various diameters of U-bends, for a vertically upward two-phase flow. The experiments were conducted for volumetric quality or gas void fraction, β, of 25%, 50%, 75%, and 95%, and superficial mixture velocity between 1–12, 2–14, 2–20, and 5–30 m/s, respectively. These conditions represent bubbly, churn, slug, and annular flow regimes. It was concluded that for a specific value of void fraction, excitation forces on bends increase with an increase in the mixture velocity. This was true for the volumetric quality values of 50%, 75%, and 95%. However, in the case of 25% void fraction, there is a large decrease in forces between 2 and 3 m/s mixture velocity. This is attributed to the fact that in this range, a transition from slug/bubbly flow to finely dispersed bubbly flow occurs. Force spectrum data demonstrated that the peak/dominant frequency shows a linear increasing trend with superficial velocity for all the observed conditions.

Hossain et al. [65] reported the effect of superficial velocities on excitation forces and dominant frequency for an upward two-phase flow in a vertical 90° elbow of internal diameter 0.0525 m (2 inch) and curvature radius of 0.0762 m (3 inch), specifically for slug and churn flows. To study the effect of superficial liquid velocity (V_{sl}), it was varied from 0.642 to 5 m/s, while maintaining a constant superficial gas velocity (V_{sg}) at 5 m/s. Furthermore, to study the effect of superficial gas velocity, it was varied from 0.5 to 9.04 m/s, while maintaining a constant superficial gas velocity at 0.642 m/s. It was observed that the magnitude of excitation force increases and the predominant frequency decreases with the increasing gas superficial velocity, while both frequency and force magnitude increase with the increasing liquid superficial velocity.

The effect of superficial velocity on force fluctuations and peak frequency was studied by Liu et al. [66], for vertically upward two-phase flow in 52.6 mm (2 inch) internal diameter pipe with a bend having a radius of 76.2 mm (3 inch). The ranges for liquid and gas phase superficial velocities investigated are 0.61–2.31 m/s and 0.1–18 m/s, respectively, covering slug, churn, annular, and bubbly flow regimes. For a fixed liquid superficial velocity, the RMS force increases monotonically with an increase in superficial velocity of gas. Moreover, the RMS force increases with liquid flow rates, but with a few exceptions, which can be attributed to flow regime transition. In the case of predominant frequency, for a constant liquid phase flow rate, the peak frequency increased to its maximum value when flow transitioned from bubbly to slug flow. A further increase in flow rate of gas phase, caused the peak frequency to decrease first for slug and churn flow regimes and increase again for annular flow regime. For a fixed flow rate of gaseous phase, the peak/dominant frequency increased with the liquid phase flow rate in general.

Experimental and numerical techniques were used by Wang et al. [67] to investigate the dynamic response of a horizontal pipe under slug flow. It was reported that these dynamic responses are created as a combined effect of the interaction between fluid and structure, and flow characteristics. The velocity of slug body has a considerable effect on the response of vibrations since this velocity affects centrifugal and Coriolis forces. The effect of slug transitional velocity was found to be intense, considering that it affects the rate of change of system properties, such as damping, stiffness, and loading.

Wang et al. [59] applied the one-way fluid structure interaction model to study the interaction of multiphase flow in a 90° pipe bend using numerical simulation. The geometry and flow parameters used were similar to Liu et al. [66]. The two-phase flow was simulated using the volume of fluid (VOF) model and realizable k-ϵ turbulence model. It was reported that at fixed liquid superficial velocity, the increasing gas velocity increases the maximum total deformation and equivalent stress, while the decreasing trend was observed with the increasing superficial liquid velocity, while maintaining a constant gas superficial velocity. The evolution of slug flow affected the position of distribution of maximum stress and deformation. The maximum value of total deformation was found at the 90° pipe bend for low liquid superficial velocities, but as the superficial velocity of liquid phase increases, the location of maximum value of total deformation was in the horizontal section of pipe. As a result, serious cyclic impact on the 90° pipe bend will be produced for higher superficial gas velocity.

In summary, fluctuation forces increase with the increase in gas superficial velocity while maintaining a constant liquid superficial velocity. Moreover, this condition is true if we reverse the conditions, where liquid superficial velocity increases while maintaining a constant gas superficial velocity. A few exceptions exist as reported, which are primarily due to flow regime transition. The peak/dominant frequency of fluctuations increases with liquid superficial velocity, but shows inconsistent behavior with the increasing gas superficial velocity, depending on flow regime change.

2.2. Effect of Pipe Geometry and Sizes

The flow behaviors in small diameter pipe bends and large diameter pipe bends are different. Schlegel et al. [68] reported that pipes can be characterized as small or large based on non-dimensional hydraulic diameter, D_H^*, as shown in Equation (2). Small pipes have D_H^* less than 18.6 and larger pipes have D_H^* greater than 40. With relevance to air-water two-phase flow, diameters < 0.0507 m correspond to D_H^* = 16.8, while diameters >0.1091 m represent D_H^* = 40. The region between these two extremes is known as the transition region and affects both large and small diameter pipes, as observed. Mishima and Ishii [69] and Schlegel et al. [68] reported that bubbly flow regime is present in small as well as large diameter pipes. Beyond the bubbly flow regime, as the superficial velocities increase, gas bubbles with larger dimensions begin to form in both small and larger diameter pipes. In small pipes, these bubbles grow and fill the entire pipe, creating long slugs, which are known as slug flow regime. In large pipes, these bubbles form cap bubbles, which are known as cap bubbly flow regime. By further increasing the velocity, the flow in smaller pipes remains as a stable slug flow, while a churn turbulent flow regime develops in pipes with a larger diameter.

$$D_H^* = \frac{D_H}{\sqrt{\frac{\sigma}{g\Delta\rho}}} \tag{2}$$

where D_H, g, σ, and $\Delta\rho$, are hydraulic diameter, gravitational acceleration, liquid phase surface tension, and difference of density between two phases, respectively.

Yih and Griffith [8] investigated three different pipe diameters (6.35, 15.9, 25.4 mm) and reported that unsteady momentum fluxes decrease as the pipe diameter increases. This is primarily due to the fact that phases are mixed better in large pipes when compared to small pipes. Overall, the pipe diameter has a very little effect on predominant frequency. The authors also reported that high transverse vibrations were observed in rectangular pipes, which were not observed in round pipes. These transverse vibrations can be attributed to the fact that rectangular pipes have low natural frequency.

Giraudeau et al. [64] investigated the effect of four different diameters (12, 15, 20, 52 mm) of U-bends on FIV for a vertically upward two-phase flow. For all conditions tested, the RMS force increased with the tube internal diameter. The increasing trend in RMS force was $D^{1.38}$, $D^{1.52}$, and $D^{1.9}$ on average for 50%, 75%, and 95% void fraction, respectively. It was reported that the peak/main frequency on force spectrum generally decreases with the tube diameter.

Chinenye-Kanu et al. [70] reported a variation in the fluctuating forces with diameter. A validated numerical modelling approach, which was used for 52.5 mm (2 inch) internal diameter pipe geometry by Hossain et al. [65] was applied to a 203.2 mm (8 inch) internal diameter pipe geometry. It was reported that peak frequencies for gas superficial velocities between 0.773 and 9.04 m/s were higher in pipes with smaller diameter compared to larger diameter pipes for similar flow conditions. Peak frequency was higher in churn flow regime for the large internal diameter pipe and in slug flow regime for the small pipes. Therefore, slug flow is critical for multiphase fluid-induced vibrations in small diameter pipes and churn flow is important when large diameter pipes are involved. The fluctuation force displayed a similar behavior in both pipe sizes by increasing monotonically with gas superficial velocity. Moreover, the study showed that for large to small pipe diameter ratio of 4, fluctuation forces were about 10× higher in the large dimeter pipe when compared to the small diameter pipe. Later, Asiegbu et al. [71] extended this study to investigate different diameter pipes (0.0525, 0.1016, 0.2032 mm). It was reported that at a constant liquid phase superficial velocity, the predominant frequency of force fluctuations increases with the increase in gas superficial velocity within the slug flow regime and drops when the flow regime transitioned into churn flow for 0.0525 mm (2 inch) and 0.2032 mm (8 inch) diameter pipe. For the case of 0.1016 mm (4 inch), the behavior of the pipe was more irregular. It was also reported that the presence of internal two-phase flow changes the natural frequency of all pipes, but the effect was more dominant in small diameter pipes when compared to large pipes.

Belfroid et al. [72] conducted experimentations to investigate the effects of FIV in large diameter pipes (i.e., 6 inch). Two different bend configurations were used with a radius of 1.5 D, one elbow and another consisted of an elbow with a U-bend upstream. The results obtained were reported to be higher than smaller diameter pipes, but were comparable with large diameter pipes (70 and 100 mm) [73,74]. A correlation to determine forces was introduced using the quasi-steady approach, as shown in Equation (3). A constant, C, of 25 and 10 is recommended to determine F_{RMS} for large and small pipes, respectively, as follows:

$$F_{RMS} = C\left(\rho_l {V_m}^2 A\right) We^{-0.4} \tag{3}$$

where ρ_l is the liquid phase density, V_m is the mixture velocity, A is the cross-sectional area of pipe, C is a constant, and We is the Weber number.

Riverin and Pettigrew [63] performed experiments on bends with different radii of curvature, R/D, (0.5, 2, 5, 7.2) and reported that R/D of the bend has a minimal effect on excitation forces. A similar conclusion regarding the minimal effect of bend radius was derived by Belfroid et al. [75]. Moreover, Cargnelutti et al. [76,77] reported the effect of radius of curvature on excitation forces. In their experiments, it was found that a larger bend radius showed greater forces when compared to a smaller bend radius. This increase in forces was attributed to the larger pressure drop in the bend with larger radius of curvature, which causes larger excitations due to the larger pressure difference. Kim et al. [78] reported that the bend radius has a direct effect on the distribution and development of local parameters. Moreover, it changes the void fraction and effects phase separation at the elbow. Yamano et al. [79,80] investigated the effect of two different radii of curvature (1 and 1.5) on FIV and reported that flow separation is continuous in short elbow and intermittent in larger elbow at the exit. Moreover, the authors observed the secondary flow behavior at the elbow, which showed that the position of high-turbulence intensity region and separation region was affected by the radius of curvature.

In summary, the excitation forces increase with the increasing diameter, while the dominant frequency decreases with the increasing diameter. The majority of these findings are based on small diameter pipes. According to Schlegel et al. [68], flow behavior in small and large pipe diameters is different. Therefore, it would be inappropriate to derive conclusions regarding FIV behavior in large pipes based on conclusions derived for small pipes and vice versa. This is also true when comparing horizontal and vertical two-phase flows. The database available on large diameter pipes is almost non-existent and further studies on their behavior are needed since the majority of practical industrial pipes are with larger diameters. In addition, it is noted that the literature on the effect of bend radius is not explored properly, and very limited variations and cases are studied. Riverin and Pettigrew [63] only studied four different bend radii and other research involved studied two different radii [76,79,80]. Therefore, there is a big gap in the body of knowledge. A further exploration on different bend radii is highly recommended, considering the dimension of bend radius effect parameters, such as void fraction, pressure drop, and phase separation. These parameters can lead to different behaviors of excitation forces and vibrations.

2.3. Effect of Flow Regimes

Two-phase flow can be divided into different flow regimes depending on their properties and appearances. Various flow regime maps are introduced over time to identify flow regimes using visual inspection and flow rates of phases involved [81,82]. Kaichiro and Ishii [69] used void fraction to identify criteria for different flow regimes and established a flow regime map with gas superficial velocity and liquid superficial velocity as horizonal and vertical coordinates. This criterion was developed for vertical two-phase flow and their results are comparable with the existing literature. More advanced methods, such as the measurement of void fraction using X-rays [83], electrical capacitance tomography [84], rotating electric field conductance gauge [85], conductivity and electrical impedance [86] are also being used to identify different flow regimes. Different flow regime visualizations are shown in Figure 4 to help in understanding and better visualizing the different types of flow regimes.

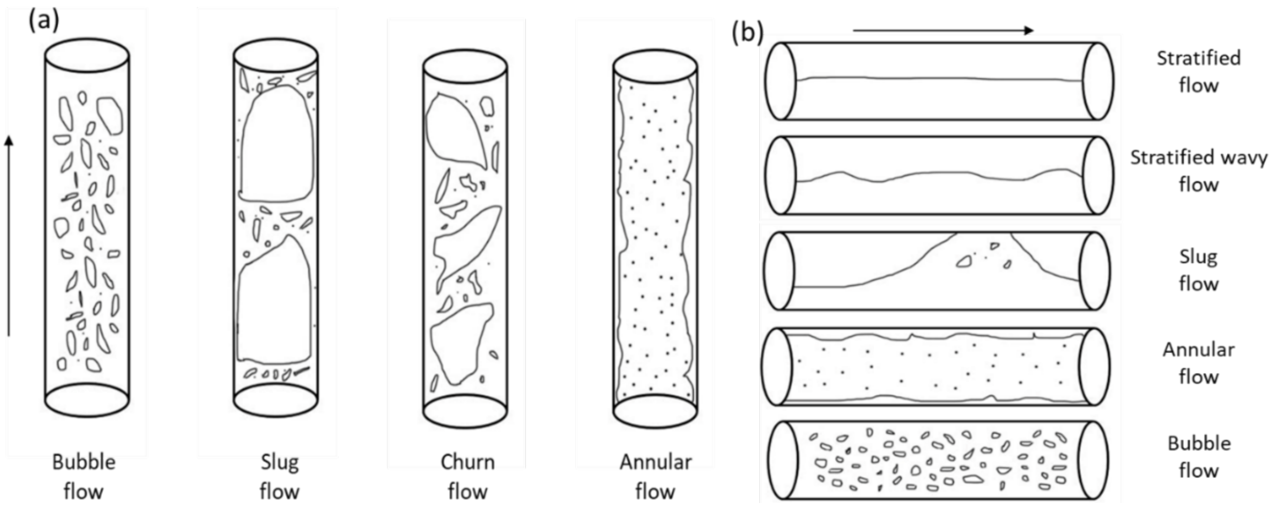

Figure 4. Flow visualization. (**a**) Flow patterns in horizontal pipe, (**b**) flow patterns in vertical pipe.

Flow regime is a critical parameter when discussing FIV in two-phase flow and different flow regimes cause different magnitudes of vibrations. Cargnelutti et al. [76,77] investigated the effect of two-phase flow on FIV in a 6-mm pipe with bend in different configurations. It was reported that slug flow showed the highest absolute forces followed by annular flow, while stratified flow showed the lowest forces. These observations were also verified in another research [75]. Cargnelutti et al. [76] developed a simple slug unit model by considering momentum fluctuation and neglecting turbulence and friction effects. This model could explain the forces generated by slug flow, but it was unable to describe forces due to annular and stratified flow regimes since no distinct slugs travel through the pipe in these flow regimes. Instead, a mixture model was presented to estimate excitation forces due to annular and stratified flows. This model is analogous to single-phase conditions, where a simple mixture momentum is considered. The results of these models were comparable to experimental results, but the accuracy can be further increased by considering parameters, such as random excitations due to turbulence, friction, gravity, and impact force.

Liu et al. [66] conducted experiments on vertically upward two-phase flow in 52.6 mm (2 inch) internal diameter pipe with a bend radius of curvature of 76.2 mm (3 inch). In this study, 36 multiphase flow cases, which include bubbly, slug, churn, and annular flow regimes, were studied. The investigated superficial velocities range of gas and liquid are 0.61–2.31 m/s and 0.1–18 m/s, respectively. For all the flow regimes, the high frequency component (>20 Hz) measured by the force sensor was insignificant. RMS values of force fluctuations were recorded in x and z directions and their peak frequency was plotted. The

RMS of force fluctuation in x and z directions are the lowest for bubbly flow regime and the value increases as the flow enters slug and churn flow regimes. In addition, it reaches the maximum value after the flow transitions into an annular flow. On the other hand, the peak frequency of force fluctuation is almost zero in bubbly flow, except for the 7-Hz peak at liquid superficial velocity of 1.78 m/s and air superficial velocity of 0.407 m/s. This random peak did not show a significant amplitude and was due to the absence of system fluctuations. When the flow transitioned into slug and churn flows, the peak frequency increased instantly to its overall maximum value due to the formation of slug bubbles in vertical section, and then decreased a little before transitioning into annular flow. The peak frequency increased again in annular flow, which was due to the disturbance wave effect. Overall, slug and churn flow regimes showed the highest peak frequencies in the range of 8 to 10 Hz.

Riverin and Pettigrew [63] also reported the behavior of force transducer signals at the elbow due to different flow regimes. Force signals are composed of regular impulses in slug flow regime, which can be attributed to the passage of liquid slugs. The force spectrum in bubbly flow regime is rather broadband due to the presence of bubbles, whereas a mixture of narrow-band and periodic components was detected in churn flow. The force signal observed in annular flow was composed of sharp impulses, which can be due to droplet entrainment. Although the majority of the literature primarily focuses on how FIV is affected by different flow regimes, it is also reported that vibration can cause a change in flow regime. Enoki et al. [87,88] observed the effect of oscillation on horizontal two-phase flow patterns in rectangular mini-channel. The flow behavior became increasingly disturbed under the influence of mechanical oscillations when compared to a stationary condition. The oscillation effect of the two-phase flow behavior was herein confirmed [88]. Moreover, it was reported than when the test section oscillated above a certain level, stratified flow would change into annular flow [88].

In conclusion, FIV behavior changes with a change in flow regime and it is a flow regime specific phenomenon. Flow-induced vibrations in slug and churn flow regimes are more intense and a further investigation is necessary, especially in annular flow regime, which appears to have received the least attention by researchers. In addition, FIV research relies on flow regime maps developed in 1970s and 1980s [82,89], and new approaches, such as flow regime map developed using machine learning algorithms or flow regimes maps for specific experimental conditions, are encouraged to be used.

2.4. Effect of Physical Properties

The effect of physical properties on excitation force exerted at 90° bend due to the two-phase flow was investigated by Tay and Thorpe [73]. It was concluded that by reducing surface tension by 32%, there was no notable effect on forces exerted on bend due to the two-phase flow. Similarly, no notable effect was observed when liquid phase viscosity was increased by 2.62%. Moreover, it was reported that liquid holdup reduces by reducing liquid surface tension, while there was no effect of liquid viscosity on liquid holdup. Furthermore, these results are supported by the empirical correlation proposed by Riverin et al. [48]. An investigation [8,73] on forces on bends was extended by Riverin et al. [48] to distinguish the effect of dimensionless parameters. The dependence of dimensionless parameters on RMS force was presented by Riverin, as shown in Equation (4). This can be further simplified to Equation (12), as shown below:

$$F_{RMS} = b\left(V_{m,}\beta, D, \rho_l, \rho_g, \sigma, \mu, g\right) \tag{4}$$

where b represents the unknown function of mentioned dimensional parameters, V_m is the mixture velocity, β is the void fraction, D is the pipe diameter, σ is the surface tension, μ is the dynamic viscosity, g is the gravitational acceleration, ρ_l and ρ_g are liquid and gas phase densities, respectively. With the use of the standard dimensional analysis from de Langre and Villard [90], Equation (4) can be written as follows:

$$\frac{F_{RMS}}{F_{stat}} = B\left(\beta, \frac{\rho_l}{\rho_g}, We, Re, Fr\right) \tag{5}$$

$$F_{stat} = \rho_l (1-\beta) {V_m}^2 \left(\pi \frac{D^2}{4}\right) \tag{6}$$

$$We = \frac{\rho_l {V_m}^2 D}{\sigma} \tag{7}$$

$$Re = \frac{\rho_l V_m D}{\mu} \tag{8}$$

$$Fr = \frac{V_m}{\sqrt{\rho_l g}} \tag{9}$$

where B only depends on dimensionless parameters and can be assumed to vary with $\frac{1}{(1-\beta)}$. Riverin who used his experimental results [48] as well as conclusions of Yih and Griffith [8] and of Tay and Thorpe [73] to study the effect of each parameter, concluded that the formulation can be extended as follows:

$$\frac{F_{RMS}}{\rho_l (1-\beta) {V_m}^2 \left(\pi \frac{D^2}{4}\right)} = \frac{B}{(1-\beta)} We^{-0.4} \tag{10}$$

This is further simplified into a dimensionless form using the Bukingham pi-theorem [91], as follows:

$$\overline{F_{RMS}} = \frac{F_{RMS}}{\rho_l {V_m}^2 \left(\pi \frac{D^2}{4}\right)} \tag{11}$$

$$\overline{F_{RMS}} = C We^{-0.4} \tag{12}$$

where C is a constant, F_{stat} is the stationary component of force, We, Re, Fr are dimensionless Weber, Reynolds, and Froude numbers, respectively. From the experimental data analysis [8,63,73], the suggested value of C is 10. Later, Cargnelutti et al. [76] tried to correlate experimental data of excitation forces on bends to the Weber number alone. The effort was unsuccessful and a reasonable accuracy was not achieved. Yih and Griffith [8] suggested the use of dimensionless parameters, such as We, Fr, and Re, while developing the correlation of excitation forces on bends. This stipulated that the incorporation of surface tension, viscosity, and gravitational effect into the F_{RMS} correlation may be important, although they appear to be unimportant. A very limited literature is available on the effects of physical properties on FIV. In addition, the available studies are focused on slug flow regime only and the findings are for limited diameter ranges. For a better explanation on the effects of physical properties in wider scale systems and various flow regimes, further research is needed.

2.5. Effect of Void Fraction

Void fraction or liquid holdup is a dimensionless parameter and can be defined as the ratio of cross-sectional area of pipe A_g occupied by vapor phase or gas to the total cross-sectional area, $A_g + A_l$. Void fraction (β) can be calculated using Equation (10) [92], as follows:

$$\beta = \frac{A_g}{A} = \frac{A_g}{A_g + A_l} \tag{13}$$

Riverin and Pettigrew [63] concluded from their experiments on multiphase flow in U-bend that excitation forces are indeed affected by the change in void fraction. In this study, the effect of excitation forces on bends at values of 25%, 50%, 75%, and 95% gas void fraction were studied. The authors reported that for a specific velocity, the excitation forces increase as void fraction increases. Maximum forces are reported between 50% to 60% gas void fraction. Beyond 60% gas void fraction, the excitation forces start to decrease. However, it is noteworthy that this effect is normally due to flow regime change. For void fractions between 50% and 60%, flow regime is normally associated with slug or churn flow, which possesses the maximum momentum flux. In addition, they are more prominent when it comes to excitation forces when compared to bubbly (25%) and annular (95%) flows.

Giraudeau et al. [64] conducted experiments to investigate flow-induced vibrations in 52 mm (2 inch) internal diameter U-bend, with a vertically upward two-phase flow. The range of gas void fraction tested during experiments are 25%, 50%, 75%, and 95%. From the force spectra data, it was concluded that the average void fraction signal corresponds to force spectra. It was reported that for a constant velocity, the excitation forces increase with void fraction until 75%, and then decrease with further increase in velocity. This behavior agrees with previous observations [63]. For 25% void fraction, forces start to increase after 3 m/s in bubbly flow. These forces are produced due to propagation of void fraction waves [93,94]. For 50% void fraction, the force increases with velocity until 7 m/s and after further increase in velocity, the forces do not show any increase, which can be explained by the transition of flow regime from unstable slug flow to bubbly flow regime. The same increasing behavior can be obtained for void fraction of 75% until velocity is increased to 14 m/s and after further increase in velocity, the force decreases. This was due to the transition of flow from unstable slug to churn flow regime. In 95% void fraction, the transition from churn to annular flow is observed at 20 m/s. Forces increase first and then start to decrease after 20 m/s due to less momentum variation in annular flow and void fraction when compared to slug and churn flow regimes.

Liu et al. [66] reported that void fraction fluctuations show a similar trend as force fluctuations, and thus it is important to determine the changes in void fraction when the two-phase flow passes through the pipe bend. Moreover, the authors observed the predominant frequency of void fraction fluctuation signals and found that for a fixed liquid superficial velocity, as superficial velocity of gas is increased from bubbly to slug flow, the predominant frequency of void fraction fluctuations reaches a maximum value, upon further increase the predominant frequency decreases in churn flow followed by an increase again in annular flow. Wang et al. [59] reported that when slug flow passes through a 90° bend, the flow regime transition affects the increase or decrease in void fraction after passing through the pipe bend. For slug flow, at a constant gas superficial velocity, void fraction decreases with the increasing liquid velocity after the slug passes through the pipe bend. However, an increasing gas superficial velocity has a minimal effect on this phenomenon.

A relationship between void fraction, liquid and gas flow rates and flow regimes based on data available in the literature [95] has been developed as illustrated in Figure 5. Notably, these data are for upward vertical flow, a flow type widely used in the study of FIV. This figure concludes the effect of void fraction on excitation forces and its relation to flow regime. For a fixed mixture velocity, the excitation forces increase as gas void fraction increases, where the maximum forces were reported to be between 50% and 75% void fraction value, and upon further increase, the excitation forces start to decrease, as shown in Figure 5. In addition, Figure 5 shows that this range covers the slug/churn flow regime, which shows maximum momentum fluctuation and, in turn, produces the highest forces. The annular and bubbly flows occur outside this range of void fraction, which shows lesser forces due to the less turbulent nature. This change is attributed to the change in flow regime as we increase the void fraction, rather than the effect of void fraction.

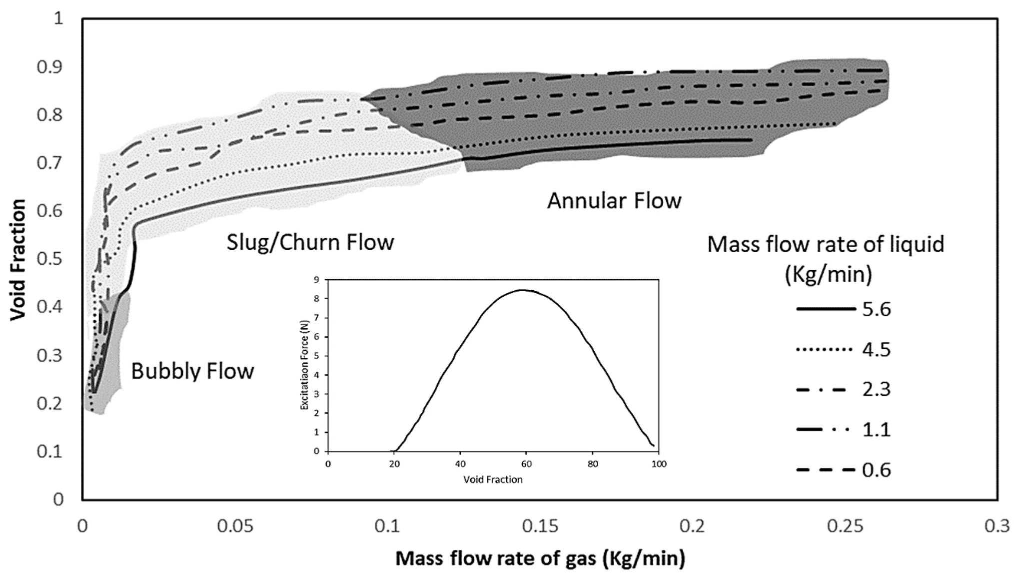

Figure 5. Relationship between void fraction with liquid and gas flowrates, and flow regimes and excitation forces.

3. Factors Affecting Dominant Frequency

Literature on two-phase flow-induced vibration is focused on the magnitude of flow forces as well as the spectrum of forces. Techniques, such as fast Fourier transform (FFT) and power spectral density (PSD) are used to identify the peak/dominant frequency. Dominant frequency carries the most energy and this frequency has the highest potential to cause damage. To avoid resonance with structural component's natural frequency, it is important to determine the dominant frequency. It can be observed from previously reported literature that this frequency lies in the range of 0–50 Hz. Moreover, the literature reports several factors that affect the dominant/peak frequency in two-phase flow, which is discussed here in detail.

Giraudeau et al. [64] analyzed the force spectrum from their experiments on U-bend with vertically upward two-phase flow. The authors reported that for the entire range of experiments, the main/dominant frequency increases linearly with superficial mixture velocity. Moreover, it was reported that the main frequency decreases with the increasing tube diameter. For 25% void fraction, narrow peaks are observed on force spectrum and as the velocity increases and flow transitions from spherical cap bubble flow to bubbly flow, the spectrum becomes wider and shows non-harmonic multiple peaks. For 50% void fraction, two harmonic frequency peaks are observed, and they increase linearly with velocity. These peaks are attributed to the passing slugs. After 7 m/s, the slug flow transition into bubbly flow and the force spectrum decrease and become wider. For 75% void fraction, one frequency peak is observed, which increases linearly with superficial mixture velocity until 14 m/s. This frequency corresponds to the slug frequency, where only one body of slug passes within a certain period. For 95% void fraction, the spectrum is considerably wider than all the other cases and increases with velocity. This can be explained by the presence of quasi-periodic excitation, which occurs in annular flow at the interface of liquid film and gas phase. Moreover, Costigan and Whalley [96] observed a few disturbances of comparable frequencies in their void fraction signals for annular flow, which contribute to the wider spectrum in annular flow. Furthermore, Giraudeau et al. [64] reported that slug frequency can be correlated to the peak frequency of force signal, and it is possible to obtain the peak frequency of force signal from slug frequency. The authors also proposed a formula, which is shown in Equation (14), to determine the peak frequency in diameter range of 20 to 52 mm for slug, unstable slug, churn, and churn/annular flows.

This formula agrees with the experimental results, except for the case of 25% void fraction, where it overestimates the value, as shown below:

$$f_0 = 0.081 \frac{V_m \sqrt{1-\beta}}{D} \tag{14}$$

where D is the tube diameter, V_m is the mixture velocity, and β is the void fraction.

Hossain et al. [65] reported the effect of superficial velocities on dominant frequency for a vertical 90° elbow of diameter 0.0525 m (2 inch) in upward vertical flow. The superficial gas velocity was varied from 0.5 to 9.04 m/s, and superficial liquid velocity was varied from 0.642 to 5 m/s, covering slug and churn flow regimes. It was reported that with the increase in superficial liquid velocity, the dominant frequency initially increases and drops with a further increase as the bubbly flow approaches. The peak frequency varied between 1 and 7 Hz. In the case of increasing gas velocity, the dominant frequency increases first to the highest value after the transition into slug flow and drops slightly with further increase toward the churn flow regime before increasing again in annular flow. In this case, the peak frequency was also varied between 1 and 7 Hz. Liu et al. [66] observed a similar behavior in their experimental study, considering that this numerical study used their experiments for validation purposes.

Asiegbu et al. [71] and Al-Hash et al. [97] reported the presence of fluid effect on natural frequencies of pipes. Asiegbu et al. found that this effect is more dominant in small diameter pipes when compared to large diameter pipes. The natural frequencies of the pipe increased with the increasing gas volume fraction. In large diameter pipes, the risk of resonance was higher since force fluctuations have low frequencies, which is equivalent with the observed low natural frequencies of large pipes. Furthermore, Al-Hash et al. [97] reported that increasing the fluid density decreases the natural frequencies of the pipe. Riverin and Pettigrew [63] performed spectral analysis of excitation forces and reported that the excitation component of forces always lies below 60 Hz, which agrees with the findings of Yih and Griffith [8]. Analysis of force spectra showed that predominant frequency increases with the increase in mixture velocity for a given void fraction. The predominant frequency is very clear for flows with intermediate void fraction values (50% and 75%). Riverin and Pettigrew [63] also proposed a formula to determine dimensionless frequency, $\overline{f}$, using Equation (15), to correlate the dimensionless force and frequency data, as follows:

$$\overline{f} = \frac{fD}{V_m} \tag{15}$$

In conclusion, the literature shows that dominant frequency increases with an increase in the mixture velocity and decreases with an increase in pipe diameter. The frequency range lies between 0 and 60 Hz. To investigate FIV successfully, the vibration of experimental flow loop should be diminished, and the frequency of experimental loop must be determined to avoid resonance. Moreover, while evaluating the natural frequency of pipe structure, the effect of added mass due to fluid should not be ignored. The literature on this phenomenon is very limited and requires further research. Furthermore, it should be noted that removing the risk of resonance does not abolish the risk of fatigue failure or excessive stress. Stress calculations are recommended to be performed in detail and the force magnitude and frequency equation can be correlated with stress to illustrate resonance and fatigue.

4. Compilation of Existing Correlations and Models for Flow-Induced Vibrations

Tables 1 and 2 summarize the existing database on FIV and the correlations developed to predict FIV in multiphase flow. The focus of past literature is on determining the magnitude of fluctuating force and force spectrum for different geometries and various flow regimes. Major existing works on FIV due to two-phase flow along with their operating conditions and limitations are listed in Table 1. The correlations developed over time by various researchers are listed in Table 2. These correlations were developed for different fluids, void fractions, pressure conditions, and geometries. The assumptions made to derive each of these equations are also listed for better understanding.

Table 1. Summary of existing database on flow-induced vibrations.

Ref.	Geometry	Diameter mm	Bend Radius	Operating Phases	Flow Regime	Flow Direction	Superficial Velocity Gas	Superficial Velocity Water	Measured Experimental Results		Simulation	Correlation Formula
									Force Magnitude	*Frequency Spectrum*		
[73,98]	90°	70	1.5 D	A-W A-5 wt% IPA A-35 wt% glycerol	Slug	Horizontal	0.38–2.87 m/s	0.2–0.7 m/s	Yes	No	No	Yes
[48,63]	T-Joint U-Bend 90°	20.6	R/d = (0.5, 2, 5, and 7.2)	A-W	Slug-Bubbly-Churn-Annular	Vertical	0.1–10.4 L/s	0.17–1.25 L/s	Yes	Yes	No	Yes
[76,77]	T-Junction T-Joint 90° Bend	6 25.4	16.5 and 25 mm Unknown	A-W	Slug-Annular -Stratified	Horizontal	0.1–30 m/s	0.05–2 m/s	Yes	No	No	Yes
[66]	90° Bend	52.5	1.5 D	A-W	Bubbly-Slug-Churn-Annular	Vertical	0.1–18 m/s	0.610–2.310 m/s	Yes	Yes	No	Yes
[64,99]	U-Bend	12 15 20 52	4 D	A-W	Bubbly-Churn-Slug-Annular -Dispersed	Vertical	0.1–30 m/s	0.7–9 m/s	Yes	Yes	No	No
[100]	90° Bend	50.8	1.5 D	A-W	Bubbly-Slug-Churn-Annular	Vertical	0.1–18 m/s	0.610–2.310 m/s	Yes	Yes	No	Yes
[72]	90° Bend U-Bend	152.4	1.5 D	A-W	Stratified-Bubbly-Slug-Annular-Dispersed	Horizonal	1–45 m/s	0.004–4 m/s	Yes	Yes	Yes	Yes
[60]	90° Bend	152.4	1.5 D	A-W	Stratified-Slug-Annular	Horizontal	-	-	No	No	Yes	No
[65]	90° Bend	52.5	1.5 D	A-W	Slug-Churn	Vertical	0.5–9.04 m/s	0.642–5 m/s	No	No	Yes	No
[71]	90° Bend	52.5 101.6 203.2	1.5 D 1.5 D 1.5 D	A-W	Slug-Churn	Vertical	0.5–9.04 m/s	0.642–5 m/s	No	No	Yes	No
[101]	90° Bend	78	Unknown	A-W	Slug	Horizontal	0.025–0.0495 Kg/s	2.48–4.97 Kg/s	No	No	Yes	No
[57]	U-Bend	6.9	1.5 D	A-W	Stratified-Slug	Vertical	-	-	No	No	Yes	No
[59]	90° Bend	52.5	1.5 D	A-W	Bubbly-Slug-Churn	Vertical	0.86–3.44 m/s	0.86–2.12 m/s	No	No	Yes	No
[102]	U-Bend	25.4	0.4 D	A-W	Bubbly-slug-wavy-annular dispersed		0.01–1.7 m/s	0.46–1.3 m/s	Yes	Yes	No	Yes

Table 2. Various correlation models developed to predict flow-induced vibrations.

References	Model	Remarks
Riverin et al. [48]	$\overline{F_{RMS}} = \frac{F_{RMS}}{\rho_l V_m^2 \left(\pi \frac{D^2}{4}\right)} = CWe^{-0.4}$	Two-phase flow is considered as a mixture with no slip between phases. Constant C needs to be determined for different conditions, C = 10 is the best fit, and C = 3.5 for slug flow in a 6-mm tube.
Tay and Thorpe [73,98]	$F = \left(\int_{in} PdA - \int_{out} PdA\right) - \frac{\partial}{\partial t}\int_{VC} \mu\rho dV - \int_{SC} \mu\rho\mu \cdot dV$ $F_x = \{\rho A j_s u_s + (P_{i,a'}A - P_o A)\} - \left\{\left(\rho A j_s \frac{d}{dt}\int_l (\cos\theta) dl\right)\right\}$ $F_y = -\left[\{-\rho A j_s u_s - (P_{i,e'}A - P_o A)\} - \left\{\left(\rho A j_s \frac{d}{dt}\int_l (\sin\theta) dl\right)\right\}\right]$	"Piston Flow Model", developed for the horizontal slug flow through a pipe bend. Flow regime was estimated from the liquid height without proper flow regime identification. Oil and gas test section was used for the experimental database.
Cargnelutti et al. [76]	Slug flow, $F = \sqrt{2}\rho_l V_{slug}^2 A$ Stratified and annular flow, $F = \sqrt{2}\rho_m V_m^2 A$	Developed for a small 6-mm tube, based on consideration of momentum change alone. Friction and gravity effects are not considered. Taylor bubble diameter is equal to the pipe diameter.
Liu et al. [66]	$F_{FS_x} = -\frac{\partial}{\partial t}\iiint_Q \left(x_f\rho_f u_{fx} + x_g\rho_g u_{gx}\right) dV$ $- \oiint_{A_{out}} \left(x_f\rho_f u_f u_f + x_g\rho_g u_g u_g\right) dS - p_{out}A$ $F_{FS_z} = -\frac{\partial}{\partial t}\iiint_Q \left(x_f\rho_f u_{fz} + x_g\rho_g u_{gz}\right) dV$ $+ \oiint_{A_{in}} \left(x_f\rho_f u_f u_f + x_g\rho_g u_g u_g\right) dS + p_{in}A - \left(\widetilde{\alpha_f}^V \rho_f + \widetilde{\alpha_g}^V \rho_g\right) gV$	Smooth transport of multiphase mixture through the pipe bend. Elbow inlet and outlet boundary pressure and void fraction signals are required as input data.
Miwa et al. [62]	It is the same model proposed by [66] with an extra term of impact force F_{IF}. $F_{IF}(t) = \frac{1}{\sqrt{2}}\rho_{2\phi}(t) A_{eff} \sqrt{\frac{kP_0}{\alpha(t)(1-\alpha(t))\rho_f}} \sqrt{\frac{2P_0}{\rho_{2\phi}(t)} \frac{L_g}{L_f}}$	Slug is considered as a homogenous two-phase mixture. Elbow inlet and outlet boundary pressure and void fraction signals are required as input data.
Belfroid et al. [72]	$F_{RMS} = C\left(\rho_l V_m{}^2 A\right) We^{-0.4}$	The correlation was developed for a 6-inch diameter pipe, C = 25 was best fit. Pressure and momentum fluctuations were considered. Quasi-steady approach was used.
Bamidele et al. [102]	$F_x = \chi_x + (p_{i.a'}A - P_o A) + Mom_x$ $F_y = \chi_y + (p_{i.e'}A - P_o A) + Mom_y$ $\Gamma_1 = \rho_f A u_f^2, \Gamma_2 = \alpha\rho_g A u_g^2 + (1-\alpha)\rho_f A u_f^2,$ Conditions for when liquid front enters the control volume $\chi_x = \Gamma_1; \chi_y = \Gamma_2,$ Conditions for when the mixture front enters the control volume $\chi_x = \Gamma_2; \chi_y = \Gamma_1,$ where Mom_x and Mom_y represent the rate of change of momentum in their respective coordinates.	A slug flow model (SFM) for time varying impact force on a horizontal bend. Assumptions made include: Incompressible flow; System is isothermal; Interface front is always vertical and at the right angle to the axis of the pipe bend. Constant fluid properties; No mass transfer between phases;Interfacial and surface stresses are negligible due to mechanical isolation of the bend; Pressure is uniform at all locations in the cross-section of the control surface.

5. Comparison of Dimensionless Forces

Riverin et al. [48] proposed an empirical correlation for dimensionless forces as shown in Equation (13). This correlation was based on experimental data for 20 mm internal diameter U-bends and tees, and appear to provide better results for void fraction values in the range of 55 to 98%. This correlation was developed on the base of model [72] for external cross flow. To develop this model, the Weber, Reynolds, and Froude numbers were considered, as shown below:

$$\overline{F_{RMS}} = \frac{F_{RMS}}{\rho_l V_m^2 \left(\pi \frac{D^2}{4}\right)} = CWe^{-0.4} \tag{16}$$

The dashed line shown in Figure 6 is drawn using Equation (16) with C of 10. This was proposed as a reasonable approximation of dimensionless forces. The dash dotted line shown in Figure 6 is drawn using C of 3.5 using Equation (16) and it is the best fit curve for slug flow regime. Giraudeau et al. [99] proposed that to be conservative, an upper bound of dimensionless forces should be defined and from their experiments on 12 to 52 mm internal diameter U-bends, $C_{\max}$ of 25 was proposed. This corresponds to the dotted line shown in Figure 6. The experimental results for 12 and 52 mm U-bends are included here, which shows that $C_{\max} = 25$ is a good approximation for upper limit. The dimensionless forces due to slug flow from experiments conducted by Cargnelutti et al. [33,34], in 6 mm internal diameter horizontal and vertical elbows for bend radii of 16.5 and 25 and the results for 25.4 mm (1 inch) internal diameter elbow, are also recorded in Figure 6. Notably, both horizontal and vertical elbows are subjected to the horizontal two-phase flow in these experiments. The overall forces on vertical elbow are higher than the horizontal elbow, which was thought to be due to gravity. Notably, forces in vertical elbow are also higher than the maximum limit introduced by Giraudeau et al. [69] at C of 25. The forces due to the 16.5 bend radius are lower than the 25 mm bend radius for the same diameter pipe, which shows that the bend radius affects the forces. Moreover, it can be observed that the forces in 25.4 mm (1 inch) pipe are higher than the 6 mm experiments. This behavior was unusual, considering that the 25.4 mm (1 inch) experiments contained more gas than the 6 mm experiments. Cargnelutti et al. [76] reported that this can also be due to the difference of stiffness of material used (glass vs. perspex). Overall, the results of Cargnelutti experiments show higher forces than the Revirin experiments and results for 25.4 mm bend are higher than $C = 10$ line. Experimental results for 20 mm internal diameter tee [42], for elbow with 70 mm diameter under the horizontal flow [98], and for 6 to 25 mm diameter vertical U-tubes [8], are also reported. All these results are in agreement with Riverin et al. [48] approximation at C of 10. Results [66] for 52.5 mm vertical elbow are also presented and these results are spread over a wide range from C of 3.51 to 25 lines. This can be attributed to the fact that 0 to 100% void fraction was considered, covering a wide range of flow conditions. The simulation results of Hossain et al. [65] for vertical elbow of 52.5 mm diameter are presented and they mostly lie between C of 10 and 25 lines. Figure 6 can serve as a database for comparison and can also be used to validate the simulation results.

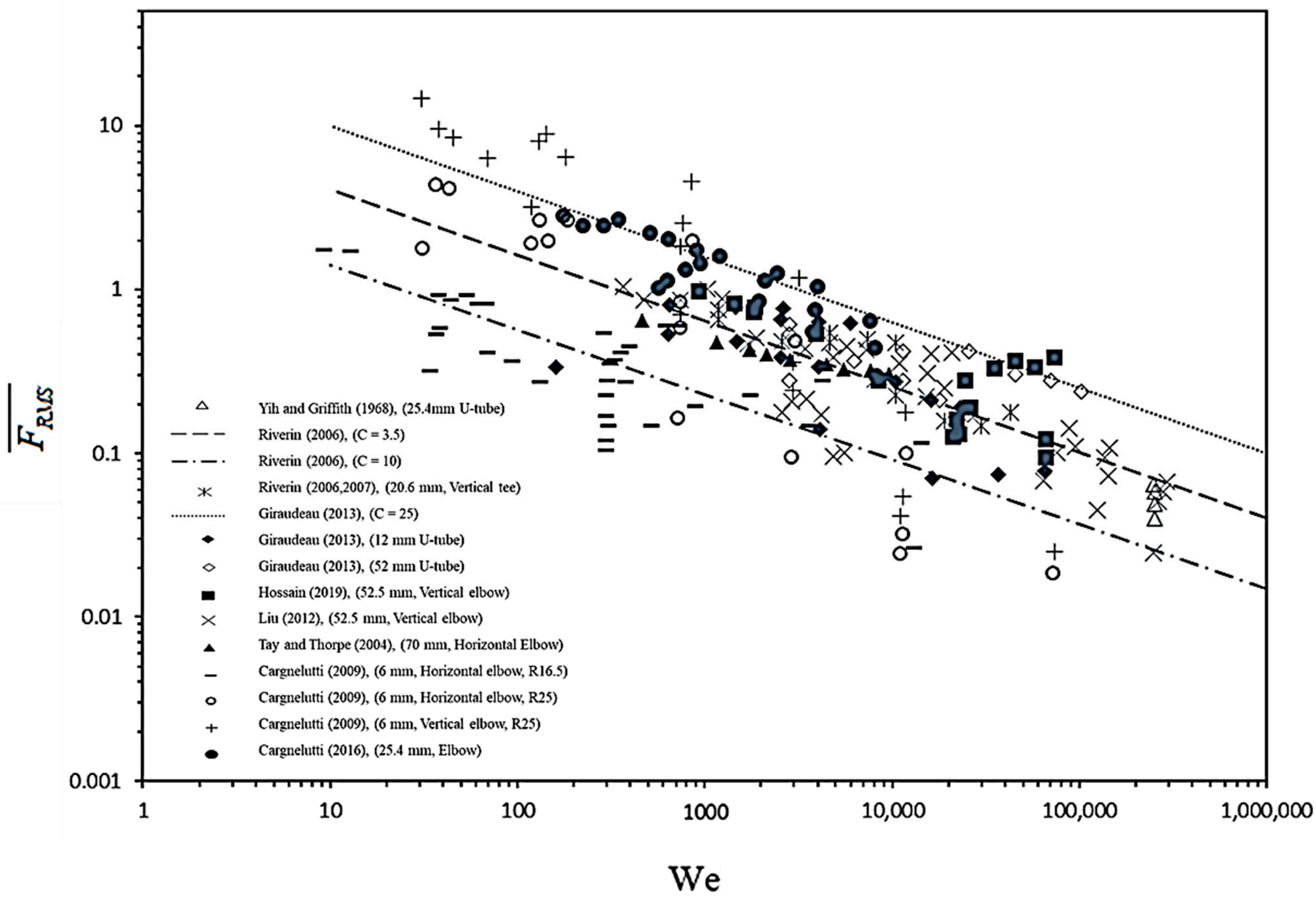

Figure 6. Comparison of dimensionless forces plotted against the Weber number [8,48,63–66,73,76,77].

6. Conclusions

In conclusion, this review article briefly introduces the background of flow-induced vibrations and its classification, followed by an in-depth review of FIV in internal two-phase flow. It is evident from the literature that for a successful investigation of FIV, the vibration of experimental flow loop should be diminished, and the natural frequency of experimental structure must be determined to avoid resonance. In addition, while evaluating the natural frequency of pipe structure, the effect of added mass due to the two-phase flow should not be ignored. It should also be noted that eliminating the risk of resonance does not remove the risk of fatigue failure or excessive stress and stress calculations should be performed in detail.

Flow-induced vibration phenomenon is flow regime dependent and most of the literature agree that forces due to slug and churn flow regimes are more intense. The effect of flow regimes should be explored further, particularly annular flow regime, which has received the least attention by researchers. Moreover, for analysis of FIV in multiphase flow, researchers are still utilizing flow regime maps developed in the 1970s and 1980s. Furthermore, additional advanced approaches are needed, such as machine learning algorithms or flow regimes maps developed for specific experimental conditions and geometries.

Geometry is considered as the major factor while considering FIV in multiphase flow. As suggested by Schlegel et al. [68], flow behavior in small and large diameter pipes is different. It can be concluded from the literature that the physical mechanism of phase distribution would be different in small and large diameter pipes and between vertical and horizontal flows. Therefore, it would be inappropriate to derive conclusions regarding FIV behavior in large pipes based on conclusions derived for small pipes and vice versa. In addition, this remark is true when comparing horizontal and vertical two-phase flows.

As an example, Nennie et al. [103] concluded that the effect of void fraction on FIV is the same for different diameter pipes. However, the authors' observations were based on small diameter pipes and may not hold true for large diameter pipes with bend in a vertically upward orientation.

Several predictive models are available in literature to predict dominant frequency and magnitude of forces due to the two-phase flow. For example, the model of Liu et al. [66] and Miwa et al. [62] can predict the magnitude and dominant frequency of forces with an average error of 30%. This model with its relatively high margin of error also needs void fraction data as an input from experiments to determine force. Therefore, to use this model to solve problems, experiments must be conducted to extract void fraction data, for specific geometry and flow conditions. The correlation by Riverin et al. [48] can also be used to calculate RMS of force fluctuations. It is recommended for void fraction value of 55% to 98% and the error margin reported is 50%. An important point to note here is that these models were developed for small diameter pipes only and the error and limitations can further increase if an attempt is made to predict for large diameter pipes. An attempt was made [72] to fit the RMS of force fluctuations for large diameter pipe (6 inch) and the prediction was further outside the original 50% error. This suggests that FIV in large diameter pipe needs to be investigated, considering there is a negligible database of FIV on large diameter pipes.

Due to the inherent complexities in interface and turbulent behavior of two-phase flow, in the past, CFD was not preferred as a tool to investigate FIV in multiphase flow. Recently, it is gaining more recognition and some previously mentioned researchers have implemented and validated their CFD results [60,65], against experimental results, to incorporate more confidence in the use of CFD for research.

7. Future Research Prospects and Challenges

The following recommendations are made to overcome the challenges in internal two-phase FIV research.

- Predictive models used to estimate FIV have many limitations, such as high margin of error, developed for a specific range of parameters and, in some cases, require experiments to collect input data for models. A study should be conducted to improve predictive models.
- Flow-induced vibrations due to multiphase flow is a flow regime dependent phenomenon. Among two-phase flow regimes, the annular flow regime needs to be explored further.
- Flow regime maps developed in the 1970s and 1980s should be replaced and new approaches should be developed.
- Research on large diameter pipes is limited and research is encouraged to widen the database.
- The effect of physical parameter, such as surface tension, viscosity, and gravity should be explored further to develop better understanding. In addition, predictive models should consider physical parameters and its effect on overall model performance.
- The effect of added mass due to two-phase flow on the natural frequency of system needs more attention.
- Developing better CFD models to study FIV. Additional comparisons of CFD and experimental results are encouraged to provide confidence to CFD users for studying multiphase FIV.

Author Contributions: Conceptualization, U.K., W.P.; writing—original draft preparation, U.K.; writing—review and editing, W.P. and N.S.; data collection, U.K.; formal analysis, U.K.; visualization, U.K.; supervision, W.P. and N.S.; data analysis, U.K. and W.P.; methodology, U.K.; project administration, U.K. and W.P.; funding acquisition W.P. and N.S. All authors have read and agreed to the published version of the manuscript.

Funding: The first and second author wish to specially acknowledge the funding for this study from Malaysia Ministry of Higher Education through Fundamental Research Grant Scheme FRGS/1/2019/TK03/UTP/02/10. All the researchers wish to thank Yayasan Universiti Teknologi PETRONAS under YUTP-15LC0-456 and YUTP-015LC0-237 for supplementary funding.

Institutional Review Board Statement: Not applicable.

Data Availability Statement: The authors declare that all data can be obtained from the corresponding author upon request.

Conflicts of Interest: The authors declare no conflict of interest.

Nomenclature

A	Area (m^2)
D	Diameter (m)
F	Force (N)
f	frequency (Hz)
$\bar{f}$	Dimensionless frequency
G	Gravitational acceleration (m/s^2)
P	Pressure (Pa)
t	Time (s)
V	Fluid Velocity (m/s)
A_g	Area occupied by gas phase (m)
A_l	Area occupied by liquid phase (m)
V_M	Mixture Velocity (m/s)
V_{sg}	Superficial Velocity of gas(m/s)
V_{sl}	Superficial Velocity of liquid (m/s)
We	Weber number
Re	Reynolds number
Fr	Froude number
β	Void fraction
μ	dynamic viscosity (Pa s)
σ	Surface tension (N/m)
ρ_l	Liquid phase density (kg/m^3)
ρ_g	Gas phase density (kg/m^3)
Subscripts	
g	Gas Phase
l	Liquid Phase
RMS	Root Mean Square
m	Liquid-Gas Mixture
sg	Superficial Gas
sl	Superficial Liquid

References

1. Triplett, K.A.; Ghiaasiaan, S.M.; Abdel-Khalik, S.I.; Sadowski, D.L. Gas–Liquid Two-Phase Flow in Microchannels Part I: Two-Phase Flow Patterns. *Int. J. Multiph. Flow* **1999**, *25*, 377–394. [CrossRef]
2. Brauner, N. Liquid-liquid two-phase flow systems. In *Modelling and Experimentation in Two-Phase Flow*; Springer: Berlin/Heidelberg, Germany, 2003; pp. 221–279. [CrossRef]
3. Ibarra, R.; Markides, C.N.; Matar, O.K. A Review of Liquid-Liquid Flow Patterns in Horizontal and Slightly Inclined Pipes. *Multiph. Sci. Technol.* **2014**, *26*, 171–198. [CrossRef]
4. Wang, W.; Li, J. Simulation of Gas–Solid Two-Phase Flow by a Multi-Scale CFD Approach—Of the EMMS Model to the Sub-Grid Level. *Chem. Eng. Sci.* **2007**, *62*, 208–231. [CrossRef]
5. Fu, F.F.; Li, J. Gas–Solid Two-Phase Flow Pattern Identification Based on Artificial Neural Network and Electrostatic Sensor Array. *Sensors* **2018**, *18*, 3522. [CrossRef]
6. Peker, S.M.; Helvaci, S.S. *Solid-Liquid Two Phase Flow*; Elsevier: Amsterdam, The Netherlands, 2008; p. 515.
7. Nirmala, G.S.; Muruganandam, L. An Experimental Study of Liquid-Solid Flow in a Circulating Fluidized Bed of Varying Liquid Viscosity. *J. Appl. Fluid Mech.* **2014**, *8*, 95–101. [CrossRef]
8. Yih, T.; Griffith, P. *Unsteady Momentum Fluxes in Two-Phase Flow and the Vibration of Nuclear Reactor Components*; Massachusetts Institute of Technology: Cambridge, MA, USA, 1968.

9. Ruspini, L.C.; Marcel, C.P.; Clausse, A. Two-Phase Flow Instabilities: A Review. *Int. J. Heat Mass Transf.* **2014**, *71*, 521–548. [CrossRef]
10. Dang, Z.; Yang, Z.; Yang, X.; Ishii, M. Experimental Study of Vertical and Horizontal Two-Phase Pipe Flow through Double 90 Degree Elbows. *Int. J. Heat Mass Transf.* **2018**, *120*, 861–869. [CrossRef]
11. O'neill, L.E.; Mudawar, I. Review of Two-Phase Flow Instabilities in Macro-and Micro-Channel Systems. *Int. J. Heat Mass Transf.* **2020**, *157*, 119738. [CrossRef]
12. Naudascher, N. *Flow-Induced Structural Vibrations*; Springer: Berlin/Heidelberg, Germany, 1972.
13. Naudascher, E.; Rockwell, D. *Practical Experiences with Flow-Induced Vibrations*; Springer: Berlin/Heidelberg, Germany, 1979.
14. Blevins, R.D. *Flow-Induced Vibration*; Van Nostrand Reinhold Co.: New York, NY, USA, 1977; ISBN 9780442208288.
15. Blevins, R.D. *Flow-Induced Vibration*, 2nd ed.; Van Nostrand Reinhold Co.: New York, NY, USA, 1990; ISBN 9780442206512.
16. Kaneko, S.; Nakamura, T.; Inada, F.; Kato, M.; Ishihara, K.; Nishihara, T.; Mureithi, N.W.; Langthje, M.A. *Flow-Induced Vibrations: Classifications and Lessons from Practical Experiences, 2nd, ed.*; Butterworth-Heinemann: Oxford, UK, 2013; ISBN 9780080983479.
17. Zhang, H.; Liu, M.K.; Fan, B.C.; Chen, Z.H.; Li, J.; Gui, M.Y. Investigations on the Effects of Vortex-Induced Vibration with Different Distributions of Lorentz Forces. *Appl. Sci.* **2017**, *7*, 61. [CrossRef]
18. Kang, H.S.; Song, K.N.; Kim, H.K.; Yoon, K.H. Axial-Flow-Induced Vibration for a Rod Supported by Translational Springs at Both Ends. *Nucl. Eng. Des.* **2003**, *220*, 83–90. [CrossRef]
19. Lee, H.B.; Lee, T.R.; Chang, Y.S. Numerical Simulation of Flow-Induced Bi-Directional Oscillations. *J. Fluids Struct.* **2013**, *37*, 220–231. [CrossRef]
20. Shiels, D.; Leonard, A.; Roshko, A. Flow-Induced Vibration of a Circular Cylinder at Limiting Structural Parameters. *J. Fluids Struct.* **2001**, *15*, 3–21. [CrossRef]
21. Ali, U.; Islam, M.; Janajreh, I.; Fatt, Y.; Alam, M.M. Flow-Induced Vibrations of Single and Multiple Heated Circular Cylinders: A Review. *Energies* **2021**, *14*, 8496. [CrossRef]
22. Quinn, E. *Vibration of Fuel Rods in Parallel Flow*; U.S. Atomic Energy Commission, Division of Technical Information: Oak Ridge, TN, USA, 1962.
23. Morita, R.; Takahashi, S.; Okuyama, K.; Inada, F.; Ogawa, Y.; Yoshiikawa, K. Evaluation of Acoustic- and Flow-Induced Vibration of the BWR Main Steam Lines and Dryer. *J. Nucl. Sci. Technol.* **2011**, *48*, 759–776. [CrossRef]
24. Pettigrew, M.J.; Taylor, C.E.; Kim, B.S. The Effects of Bundle Geometry on Heat Exchanger Tube Vibration in Two-Phase Cross Flow. *J. Press. Vessel Technol. Trans. ASME* **2001**, *123*, 414–420. [CrossRef]
25. Pettigrew, M.J.; Knowles, G.D. Some Aspects of Heat-Exchanger Tube Damping in Two-Phase Mixtures. *J. Fluids Struct.* **1997**, *11*, 929–945. [CrossRef]
26. Wang, J.S.; Fan, D.; Lin, K. A Review on Flow-Induced Vibration of Offshore Circular Cylinders. *J. Hydrodyn.* **2020**, *32*, 415–440. [CrossRef]
27. Paidoussis, M.P. Vibration of Cylindrical Structures Induced by Axial Flow. *J. Eng. Ind.* **1974**, *96*, 547–552. [CrossRef]
28. Pettigrew, M.J.; Taylor, C.E. Two-Phase Flow-Induced Vibration: An Overview (Survey Paper). *J. Press. Vessel Technol.* **1994**, *116*, 233–253. [CrossRef]
29. Gorman An Analytical and Experimental Investigation of the Vibration of Cylindrical Reactor Fuel Elements in Two-Phase Parallel Flow. *Nucl. Sci. Eng.* **1971**, *44*, 277–290. [CrossRef]
30. Pettigrew, M.J.; Gorman, D.J. *Experimental Studies on Flow Induced Vibration to Support Steam Generator Design, Part 1: Vibration of a Heated Cylinder in Two-Phase Axial Flow*; Atomic Energy of Canada Limited: Laurentian Hills, ON, Canada, 1973.
31. Carlucci, L.N.; Brown, J.D. Experimental Studies of Damping and Hydrodynamic Mass of a Cylinder in Confined Two-Phase Flow. *J. Vib. Acoust. Stress Reliab. Des.* **1983**, *105*, 83–89. [CrossRef]
32. Carlucci, L.N. Damping and Hydrodynamic Mass of a Cylinder in Simulated Two-Phase Flow. *J. Mech. Des.* **1980**, *102*, 597–602. [CrossRef]
33. Khushnood, S.; Khan, Z.M.; Malik, M.A.; Koreshi, Z.U.; Khan, M.A. A Review of Heat Exchanger Tube Bundle Vibrations in Two-Phase Cross-Flow. *Nucl. Eng. Des.* **2004**, *230*, 233–251. [CrossRef]
34. Mitra, D.; Dhir, V.K.; Catton, I. Fluid-Elastic Instability in Tube Arrays Subjected to Air-Water and Steam-Water Cross-Flow. *J. Fluids Struct.* **2009**, *25*, 1213–1235. [CrossRef]
35. Nakamura, T.; Fujita, K.; Kawanishi, K.; Yamaguchi, N.; Tsuge, A. Study on the Vibrational Characteristics of a Tube Array Caused by Two-Phase Flow—Part 1: Random Vibration. *J. Press. Vessel Technol.* **1992**, *114*, 472–478. [CrossRef]
36. Sasakawa, T.; Serizawa, A.; Kawara, Z. Fluid-Elastic Vibration in Two-Phase Cross Flow. *Exp. Therm. Fluid Sci.* **2005**, *29*, 403–413. [CrossRef]
37. Zhang, C.; Pettigrew, M.J.; Mureithi, N.W. Vibration Excitation Force Measurements in a Rotated Triangular Tube Bundle Subjected to Two-Phase Cross Flow. *J. Press. Vessel Technol.* **2007**, *129*, 21–27. [CrossRef]
38. Wang, Z.; Fan, D.; Triantafyllou, M.S. Illuminating the Complex Role of the Added Mass during Vortex Induced Vibration. *Phys. Fluids* **2021**, *33*, 085120. [CrossRef]
39. Pettigrew, M.J.; Taylor, C.E.; Fisher, N.J.; Yetisir, M.; Smith, B.A.W. Flow-Induced Vibration: Recent Findings and Open Questions. *Nucl. Eng. Des.* **1998**, *185*, 249–276. [CrossRef]
40. Konstantinidis, E. Cross-Flow-Induced Vibration of an Elastic Plate. *Fluids* **2021**, *6*, 82. [CrossRef]

41. Garg, H.; Soti, A.K.; Bhardwaj, R. Vortex-Induced Vibration and Galloping of a Circular Cylinder in Presence of Cross-Flow Thermal Buoyancy. *Phys. Fluids* **2019**, *31*, 113603. [CrossRef]
42. Chen, W.; Ji, C.; Williams, J.; Xu, D.; Yang, L.; Cui, Y. Vortex-Induced Vibrations of Three Tandem Cylinders in Laminar Cross-Flow: Vibration Response and Galloping Mechanism. *J. Fluids Struct.* **2018**, *78*, 215–238. [CrossRef]
43. Sawadogo, T.; Mureithi, N. Time Domain Simulation of the Vibration of a Steam Generator Tube Subjected to Fluidelastic Forces Induced by Two-Phase Cross-Flow. *J. Press. Vessel Technol. Trans. ASME* **2013**, *135*, 030905. [CrossRef]
44. Sadek, O.; Mohany, A.; Hassan, M. Numerical Investigation of the Cross Flow Fluidelastic Forces of Two-Phase Flow in Tube Bundle. *J. Fluids Struct.* **2018**, *79*, 171–186. [CrossRef]
45. Chen, S.S. Out-of-Plane Vibration and Stability of Curved Tubes Conveying Fluid. *J. Appl. Mech.* **1973**, *40*, 362–368. [CrossRef]
46. Crawford, N.M.; Cunningham, G.; Spence, S.W.T. An Experimental Investigation into the Pressure Drop for Turbulent Flow in 90° Elbow Bends. *Proc. Inst. Mech. Eng. Part E J. Process. Mech. Eng.* **2007**, *221*, 77–88. [CrossRef]
47. Weaver, D.S.; Ziada, S.; Au-Yang, M.K.; Chen, S.S.; Païdoussis, M.P.; Pettigrew, M.J. Flow-Induced Vibrations in Power and Process Plant Components—Progress and Prospects. *J. Press. Vessel Technol. Trans. ASME* **2000**, *122*, 339–348. [CrossRef]
48. Riverin, J.L.; de Langre, E.; Pettigrew, M.J. Fluctuating Forces Caused by Internal Two-Phase Flow on Bends and Tees. *J. Sound Vib.* **2006**, *298*, 1088–1098. [CrossRef]
49. Bamidele, O.E.; Ahmed, W.H.; Hassan, M. Flow Induced Vibration of Separated Two-Phase Flow Due to Restricting Orifice. *Int. Conf. Fluid Flow Heat Mass Transf.* **2019**, *38*, 1–10. [CrossRef]
50. Wang, S.; Shoji, M. Fluctuation Characteristics of Two-Phase Flow Splitting at a Vertical Impacting T-Junction. *Int. J. Multiph. Flow* **2002**, *28*, 2007–2016. [CrossRef]
51. Zhu, H.; Gao, Y.; Zhao, H. Experimental Investigation on the Flow-Induced Vibration of a Free-Hanging Flexible Riser by Internal Unstable Hydrodynamic Slug Flow. *Ocean Eng.* **2018**, *164*, 488–507. [CrossRef]
52. Ali, F.; Bilal, M.; Sheikh, N.A.; Khan, I.; Nisar, K.S. Two-Phase Fluctuating Flow of Dusty Viscoelastic Fluid between Non-Conducting Rigid Plates with Heat Transfer. *IEEE Access* **2019**, *7*, 123299–123306. [CrossRef]
53. Emmerson, P.; Lewis, M.; Barton, N. Improving Boundary Conditions For Multiphase CFD Predictions of Slug Flow Induced Forces. In Proceedings of the 17th International Conference on Multiphase Production Technology, Cannes, France, 10–12 June 2015.
54. Araújo, J.D.P.; Miranda, J.M.; Campos, J.B.L.M. CFD Study of the Hydrodynamics of Slug Flow Systems: Interaction between Consecutive Taylor Bubbles. *Int. J. Chem. React. Eng.* **2014**, *13*, 541–549. [CrossRef]
55. Ban, S.; Pao, W.; Nasif, M.S. Numerical Simulation of Two-Phase Flow Regime in Horizontal Pipeline and Its Validation. *Int. J. Numer. Methods Heat Fluid Flow* **2018**, *28*, 1279–1314. [CrossRef]
56. Nichita, B.A.; Zun, I. A Volume of Fluid Method for Modeling of Gas-Liquid Interface. *J. Fluids Eng.* **2015**, *132*, 081302. [CrossRef]
57. De Moerloose, L.; Degroote, J. A Study of the Vibration of a Horizontal U-Bend Subjected to an Internal Upwards Flowing Air–Water Mixture. *J. Fluids Struct.* **2020**, *93*, 102883. [CrossRef]
58. Mohmmed, A.O.; Al-Kayiem, H.H.; Osman, A.B.; Sabir, O. One-Way Coupled Fluid–Structure Interaction of Gas–Liquid Slug Flow in a Horizontal Pipe: Experiments and Simulations. *J. Fluids Struct.* **2020**, *97*, 103083. [CrossRef]
59. Wang, Z.; He, Y.P.; Li, M.Z.; Qiu, M.; Huang, C.; Liu, Y.D.; Wang, Z. Fluid—Structure Interaction of Two-Phase Flow Passing Through 90° Pipe Bend Under Slug Pattern Conditions. *China Ocean Eng.* **2021**, *35*, 914–923. [CrossRef]
60. Mack, A.; Joshi, H.; Belfroid, S. Numerical Rebuilding of Dynamic Instabilities and Forces in Multiphase Pipe Bend Flow. *Int. J. Comput. Methods Exp. Meas.* **2018**, *6*, 358–372. [CrossRef]
61. Liang, Z.; Guo, C.; Wang, C. The Connection between Flow Pattern Evolution and Vibration in 90-Degree Pipeline: Bidirectional Fluid-Structure Interaction. *Energy Sci. Eng.* **2022**, *10*, 308–323. [CrossRef]
62. Miwa, S.; Mori, M.; Hibiki, T. Two-Phase Flow Induced Vibration in Piping Systems. *Prog. Nucl. Energy* **2015**, *78*, 270–284. [CrossRef]
63. Riverin, J.L.; Pettigrew, M.J. Vibration Excitation Forces Due to Two-Phase Flow in Piping Elements. *J. Press. Vessel Technol. Trans. ASME* **2007**, *129*, 7–13. [CrossRef]
64. Giraudeau, M.; Mureithi, N.W.; Pettigrew, M.J. Two-Phase Flow-Induced Forces on Piping in Vertical Upward Flow: Excitation Mechanisms and Correlation Models. *J. Press. Vessel Technol. Trans. ASME* **2013**, *135*, 1–16. [CrossRef]
65. Hossain, M.; Chinenye-Kanu, N.M.; Droubi, G.M.; Islam, S.Z. Investigation of Slug-Churn Flow Induced Transient Excitation Forces at Pipe Bend. *J. Fluids Struct.* **2019**, *91*, 102733. [CrossRef]
66. Liu, Y.; Miwa, S.; Hibiki, T.; Ishii, M.; Morita, H.; Kondoh, Y.; Tanimoto, K. Experimental Study of Internal Two-Phase Flow Induced Fluctuating Force on a 90° Elbow. *Chem. Eng. Sci.* **2012**, *76*, 173–187. [CrossRef]
67. Wang, L.; Yang, Y.; Li, Y.; Wang, Y. Dynamic Behaviours of Horizontal Gas-Liquid Pipes Subjected to Hydrodynamic Slug Flow: Modelling and Experiments. *Int. J. Press. Vessel. Pip.* **2018**, *161*, 50–57. [CrossRef]
68. Schlegel, J.P.; Miwa, S.; Chen, S.; Hibiki, T.; Ishii, M. Experimental Study of Two-Phase Flow Structure in Large Diameter Pipes. *Exp. Therm. Fluid Sci.* **2012**, *41*, 12–22. [CrossRef]
69. Kaichiro, M.; Ishii, M. Flow Regime Transition Criteria for Upward Two-Phase Flow in Vertical Tubes. *Int. J. Heat Mass Transf.* **1984**, *27*, 723–737. [CrossRef]
70. Chinenye-Kanu, N.M.; Hossain, M.; Droubi, M.G.; Islam, S.Z. Numerical Investigation of Two-Phase Flow Induced Local Fluctuations and Interactions of Flow Properties through Elbow. *Lect. Notes Mech. Eng.* **2019**, *2019*, 124–141. [CrossRef]

71. Asiegbu, N.M.; Hossain, M.; Droubi, G.M.; Islam, S.Z. Investigation of the Effects of Pipe Diameter of Internal Multiphase Flow on Pipe Elbow Vibration and Resonance. *Proc. Inst. Mech. Eng. Part E J. Process. Mech. Eng.* **2022**, *2022*, 095440892211155. [CrossRef]
72. Belfroid, S.P.; Nennie, E.; Lewis, M. Multiphase Forces on Bends—Large Scale 6″ Experiments. In Proceedings of the SPE Annual Technical Conference and Exhibition, Dubai, United Arab Emirates, 26–28 September 2016.
73. Tay, B.L.; Thorpe, R.B. Effects of Liquid Physical Properties on the Forces Acting on a Pipe Bend in Gas-Liquid Slug Flow. *Chem. Eng. Res. Des.* **2004**, *82*, 344–356. [CrossRef]
74. Nennie, E.D.; Belfroid, S.P.C.; van Bokhorst, E.; Remans, D. Multiphase Fluid Structure Interaction in Pipe Systems with Multiple Bends. In Proceedings of the 10th International Conference on Flow-Induced Vibration, Dublin, Ireland, 3–6 July 2012; TNO Publications: The Hague, The Netherlands.
75. Belfroid, S.P.C.; Cargnelutti, M.F.; Schiferli, W.; Van Osch, M. Forces on Bends and T-Joints Due to Multiphase Flow. *Am. Soc. Mech. Eng. Fluids Eng. Div. FEDSM* **2010**, *3*, 613–619. [CrossRef]
76. Cargnelutti, M.F.; Belfroid, S.P.C.; Schiferli, W.; Van Osch, M. Two-Phase Flow-Induced Forces on Bends in Small Scale Tubes. *J. Press. Vessel. Technol.* **2009**, *132*, 1–9.
77. Cargnelutti, M.F.; Belfroid, S.P.C.; Schiferli, W.; Van Osch, M. Multiphase Fluid Structure Interaction in Bends and T-Joints. In Proceedings of the ASME 2010 Pressure Vessels and Piping Division/K-PVP Conference, Bellevue, DC, USA, 18–22 July 2016; pp. 1–8.
78. Kim, S.; Park, J.H.; Kojasoy, G.; Kelly, J.M.; Marshall, S.O. Geometric Effects of 90-Degree Elbow in the Development of Interfacial Structures in Horizontal Bubbly Flow. *Nucl. Eng. Des.* **2007**, *237*, 2105–2113. [CrossRef]
79. Yamano, H.; Tanaka, M.; Murakami, T.; Iwamoto, Y.; Yuki, K.; Sago, H.; Hayakawa, S. Unsteady Elbow Pipe Flow to Develop a Flow-Induced Vibration Evaluation Methodology for Japan Sodium-Cooled Fast Reactor. *J. Nucl. Sci. Technol.* **2011**, *48*, 677–687. [CrossRef]
80. Yamano, H.; Tanaka, M.A.; Kimura, N.; Ohshima, H.; Kamide, H.; Watanabe, O. Development of Flow-Induced Vibration Evaluation Methodology for Large-Diameter Piping with Elbow in Japan Sodium-Cooled Fast Reactor. *Nucl. Eng. Des.* **2011**, *241*, 4464–4475. [CrossRef]
81. Taitel, Y.; Barnea, D.; Dukler, A.E. Modelling Flow Pattern Transitions for Steady Upward Gas-Liquid Flow in Vertical Tubes. *AIChE J.* **1980**, *26*, 345–354. [CrossRef]
82. Mandhane, J.M.; Gregory, G.A.; Aziz, K. A Flow Pattern Map for Gas—Liquid Flow in Horizontal Pipes. *Int. J. Multiph. Flow* **1974**, *1*, 537–553. [CrossRef]
83. Jones, O.C.; Zuber, N. The Interrelation between Void Fraction Fluctuations and Flow Patterns in Two-Phase Flow. *Int. J. Multiph. Flow* **1975**, *2*, 273–306. [CrossRef]
84. Wang, H.X.; Zhang, L.F. Identification of Two-Phase Flow Regimes Based on Support Vector Machine and Electrical Capacitance Tomography. *Meas. Sci. Technol.* **2009**, *20*, 114007. [CrossRef]
85. Merilo, M.; Dechene, R.L.; Cichowlas, W.M. Void Fraction Measurement With a Rotating Electric Field Conductance Gauge. *J. Heat Transfer* **1977**, *99*, 330–332. [CrossRef]
86. Juliá, J.E.; Liu, Y.; Paranjape, S.; Ishii, M. Upward Vertical Two-Phase Flow Local Flow Regime Identification Using Neural Network Techniques. *Nucl. Eng. Des.* **2008**, *238*, 156–169. [CrossRef]
87. Enoki, K.; Ono, M.; Okawa, T.; Kristiawan, B.; Wijayanta, A.T. Water Flow Boiling Heat Transfer in Vertical Minichannel. *Exp. Therm. Fluid Sci.* **2020**, *117*, 110147. [CrossRef]
88. Enoki, K.; Ono, M.; Okawa, T.; Akisawa, A.; Mori, H.; Kristiawan, B.; Wijayanta, A.T. Two-Phase Flow Regimes of Refrigerant R134a in an Oscillating Horizontal Rectangular Minichannel Conduit. *Int. J. Refrig.* **2020**, *118*, 261–268. [CrossRef]
89. Taitel, Y.; Dukler, A.E. A Model for Predicting Flow Regime Transitions in Horizontal and near Horizontal Gas-liquid Flow. *AIChE J.* **1976**, *22*, 47–55. [CrossRef]
90. De Langre, E.; Villard, B. An Upper Bound on Random Buffeting Forces Caused by Two-Phase Flows across Tubes. *J. Fluids Struct.* **1998**, *12*, 1005–1023. [CrossRef]
91. Buckingham, E. On Physically Similar Systems; Illustrations of the Use of Dimensional Equations. *Phys. Rev.* **1914**, *4*, 345. [CrossRef]
92. Thome, J.R.; Cioncolini, A. *Encyclopedia of Two-Phase Heat Transfer and Flow I*; Chapter 4: Void Fraction; World Scientific: Singapore, 2015; pp. 85–112. [CrossRef]
93. Park, J.W.; Drew, D.A.; Lahey, R.T. The Measurement of Void Waves in Bubbly Two-Phase Flows. *Nucl. Eng. Des.* **1994**, *149*, 37–52. [CrossRef]
94. Sun, B.; Yan, D.; Zhang, Z. The Instability of Void Fraction Waves in Vertical Gas-Liquid Two-Phase Flow. *CNSNS* **1999**, *4*, 181–186. [CrossRef]
95. Ghajar, A.J.; Bhagwat, S.M. *Frontiers and Progress in Multiphase Flow I*; Springer: Berlin/Heidelberg, Germany, 2014; ISBN 9783319043586.
96. Costigan, G.; Whalley, P.B. Slug Flow Regime Identification from Dynamic Void Fraction Measurements in Vertical Air-Water Flows. *Int. J. Multiph. Flow* **1997**, *23*, 263–282. [CrossRef]
97. Al-Hash, Z.I.; Al-Kayi, H.H.; Hasan, F.; Mohmmedd, A. Effect of Various Fluid Densities on Vibration Characteristics in Variable Cross-Section Pipes. *J. Appl. Sci.* **2014**, *14*, 2054–2060. [CrossRef]

98. Tay, B.L.; Thorpe, R.B. Hydrodynamic Forces Acting on Pipe Bends in Gas-Liquid Slug Flow. *Chem. Eng. Res. Des.* **2014**, *92*, 812–825. [CrossRef]
99. Giraudeau, M.; Mureithi, N.W.; Pettigrew, M.J. Two-Phase Flow Excitation Forces on a Vertical U-Bend Tube. In Proceedings of the ASME 2011 Pressure Vessels and Piping Conference, Baltimore, MD, USA, 17–21 July 2011; pp. 103–111.
100. Miwa, S.; Liu, Y.; Hibiki, T.; Ishii, M.; Kondo, Y.; Morita, H.; Tanimoto, K. Study of Unsteady Gas-Liquid Two-Phase Flow Induced Force Fluctuation (Part 2: Horizontal-Downward Two-Phase Flow). *Trans. JSME* **2014**, *80*, TEP0046. [CrossRef]
101. Gourma, M.; Verdin, P.G. Nature and Magnitude of Operating Forces in a Horizontal Bend Conveying Gas-Liquid Slug Flows. *J. Pet. Sci. Eng.* **2020**, *190*, 107062. [CrossRef]
102. Bamidele, O.E.; Ahmed, W.H.; Hassan, M. Characterizing Two-Phase Flow-Induced Vibration in Piping Structures with U-Bends. *Int. J. Multiph. Flow* **2022**, *151*, 104042. [CrossRef]
103. Nennie, E.; Belfroid, S.P.C.; O'Mahoney, T.S.D. Omae2013-10543 Validation of CFD and Simplified Models with Experimental Data for Multiphase Flow in Bends. In *International Conference on Offshore Mechanics and Arctic Engineering*; American Society of Mechanical Engineers: New York, NY, USA, 2013; pp. 1–10.